Transport of Momentum in the SOL of ASDEX Upgrade

F. Mehlmann[1], C. Ionita[1], V. Naulin[2], J.J. Rasmussen[2], H.W. Müller[3], N. Vianello[4], Ch. Maszl[1], V. Rohde[3], M. Zuin[4], R. Cavazzana[4], M. Maraschek[3], R. Schrittwieser[1], ASDEX Upgrade Team[3]

[1]*Association EURATOM/ÖAW, Institute for Ion Physics and Applied Physics, University of Innsbruck, Austria*

[2]*Association EURATOM/RISØ-Technical University of Denmark, Roskilde, Denmark*

[3]*Max-Planck-Institut für Plasmaphysik, EURATOM Association, Garching, Germany*

[4]*Consorzio RFX, Associazione Euratom-ENEA sulla Fusione, Padova, Italy*

Abstract: Radial transport of poloidal momentum in the scrape-off layer (SOL) of ASDEX Upgrade was investigated. A reciprocating probe was used with a probe head containing six Langmuir probes with which the poloidal and radial electric field components and the density were determined. Separating all quantities into stationary and fluctuating parts, four components of the momentum transport were evaluated separately. We see a distinct change in behaviour between L- and H-mode discharges. Particularly the direction of momentum flux at the probe location is opposite between L- and H-mode.

1. Introduction

In magnetized plasmas turbulence is the dominating mechanism for transport of mass, energy and momentum, across the magnetic field. Radial flux of poloidal momentum has recently become a highly interesting topic in context with the general problem of edge plasma transport, also in connection with edge localized modes (ELMs). In particular the variation of poloidal and toroidal rotation speed before and after a type I ELM is an important question. During an ELM the angular velocity decreases, after it the plasma speeds up again [1]. The observed variation of the strike point during ELMs and the thereby triggered release of plasma current could be related to this problem [2].

2. Experimental results and discussion

We have used a special probe head on the midplane manipulator in the far SOL during ASDEX Upgrade L-mode and H-mode discharges; see [3,4] for a detailed description. Six graphite pins serve to determine ion density n_i and poloidal and radial electric field components, $E_{\theta,r}$, simultaneously; $n \cong n_i$ is taken as the plasma density. The respective floating pins have a distance of 10 mm in poloidal direction and of 3 mm in radial direction. To derive the electric field we have to assume that the electron temperature, T_e, is equal on all probe positions.

The following relevant transport quantities can be derived: (i) radial particle flux $\Gamma_r = \tilde{n}\tilde{v}_r = \tilde{n}\tilde{E}_\theta / B_\phi$, (ii) Reynolds stress $\mathcal{Re} = n_0 \tilde{v}_r \tilde{v}_\theta = n_0 \tilde{E}_\theta \tilde{E}_r / B_\phi^2$, (iii) radial flux of poloidal momentum $M_r = n v_r v_\theta = n E_\theta E_r / B_\phi^2$.

Here $v_{r,\theta}$ are the radial and poloidal velocity components, respectively, B_ϕ is the toroidal magnetic field. With n and $v_{r,\theta}$ being defined as $X = X_0 + X_{\mathrm{fl}}$, the momentum flux can be split up into four contributions [5]: $M_r = \mathcal{Re} + v_{\theta,0}\Gamma_r + n_{\mathrm{fl}}\, v_{r,\mathrm{fl}}\, v_{\theta,\mathrm{fl}} + n_0\, v_{r,\mathrm{fl}}\, v_{\theta,0}$. We see that the first term of M_r contains the Reynolds stress, and the second one is the convective momentum flux containing the radial particle flux. The third term is composed of only fluctuating quantities. The fourth term of M_r does not contribute on average, because if the average is taken over the entire time, we see that $\langle n_0\, v_{r,\mathrm{fl}}\, v_{\theta,0}\rangle = n_0\, v_{\theta,0}\, \langle v_{r,fl}\rangle = 0$.

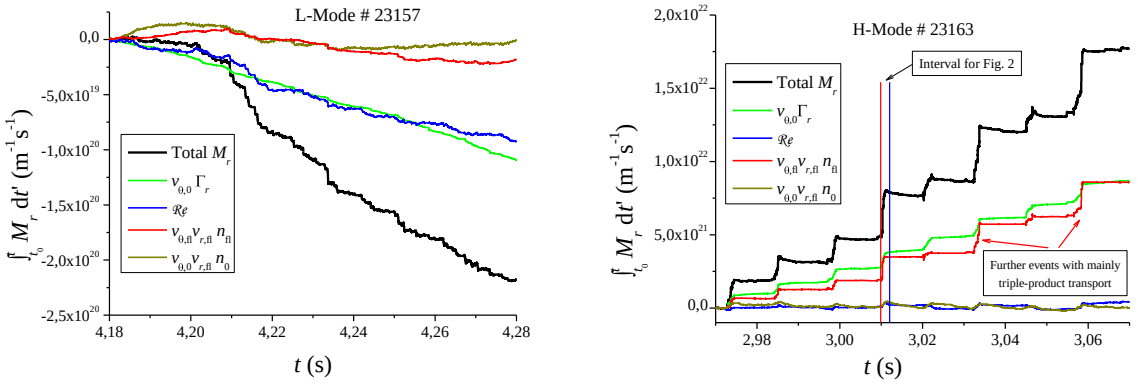

(a) **(b)**

Fig. 1. Integrated radial flux of poloidal momentum during the observation interval, total momentum (black line), the other lines show the parameters listed; (a) during L-mode discharge #23157, (b) during H-mode #23163; the red and blue vertical lines delimit the time interval of the single ELM shown in Fig. 2.

Fig. 1 shows the integrated momentum flux $\int_{t_0}^{t} M_r \, \mathrm{d}t'$ during an L-mode discharge (a) and an H-mode discharge (b).

The main parameters of the purely ohmic L-mode discharge #23157 (no rf heating) were (Fig. 1a): Plasma current I_{pl}= 0,80 MA, electron density n_e= 4,9·10^{19} m^{-3}, total magnetic field B_t = –2,48 T, safety factor q_{95}= 5,26. The distance of the front side of the probe head to the lasts close flux surface (LCFS) was in this case 45 mm.

In the absence of external momentum input by beams the momentum should basically be generated from turbulence in the form of residual stresses (asymmetry flows) by the Reynolds stress and direct interaction with the SOL flows. Thus the term $\mathcal{Re}$ will, together with the convective part, dominate the momentum flux. We see that $\mathcal{Re}$ and the convective momen-

tum transport term $v_{\theta,0}\Gamma_r$ have about the same size and dominate as expected.

In H-mode discharge #23163 (Fig. 1b) we see the time interval 2,97 ≤ t ≤ 3,02 s, during which the reciprocating probe head was on a stable radial position. The main plasma parameters of this discharge were: I_{pl} = 0,80 MA, n_e = 6,7·10^{19} m^{-3}, B_t = –2,48 T, q_{95} = 5,25. The neutral beam injection (NBI) power was P_{NBI} = 5,1 MW for 0,895 ≤ t ≤ 4,843 s and the power of ICRH heating was P_{ICRH} = 3,7 MW during the entire discharge. Here the distance of the front side of the probe head to the lasts close flux surface (LCFS) was 38 mm.

Fig. 1b shows the flux of poloidal momentum. We see the typical stepwise increase of the transported momentum, where each steep step indicates an ELM whereas during the inter-ELM intervals the flux is almost zero or even slightly negative. The total flux of momentum is almost two orders of magnitude larger than in the L-mode. We point out that with this probe only a localized determination of the quantities is possible.

In this case the particle transport term $v_{\theta,0}\Gamma_r$ (green line), and the triple fluctuating term $n_{\mathrm{fl}}\, v_{r,\mathrm{fl}}\, v_{\theta,\mathrm{fl}}$ (red line) are of comparable size and dominate on the average, whereas the Reynolds stress $\mathcal{R}\!e$ is small and fluctuating. So it does not contribute considerably to the total flux.

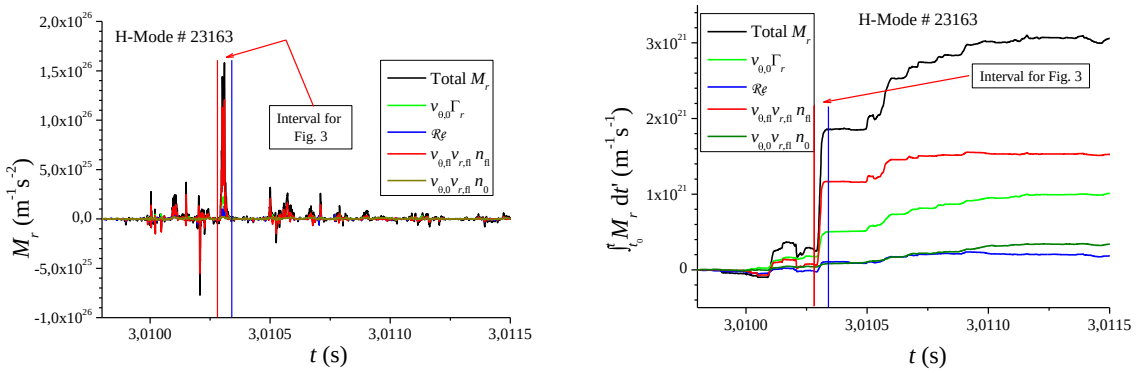

Fig. 2. Instantaneous (a) and integrated (b) momentum flux during the ELM time interval delimited by the red and blue vertical line in Fig. 2; total momentum (black line), the other lines show the parameters listed. The red and blue vertical lines delimit the time interval of the single ELM filament shown in Fig. 3.

Fig. 2 shows a close up of one ELM during H-mode discharge #23163. In Fig. 1b this time interval is delimited by a red and blue vertical line. The filamentary structure of this ELM is visible in detail, and we discern that there is one particularly strong flux event for t ≅ 3,0103 s. Here it turns out that the triple fluctuating term $n_{\mathrm{fl}}\, v_{r,\mathrm{fl}}\, v_{\theta,\mathrm{fl}}$ leads to a considerably larger momentum flux than the particle transport term $v_{\theta,0}\Gamma_r$. This is also seen in other ELMs, as indicated in Fig. 1b. Fig. 3 shows a further close up of this strong transport event to elucidate its fine-structure. In Fig. 2 this time interval is delimited by a red and blue vertical line.

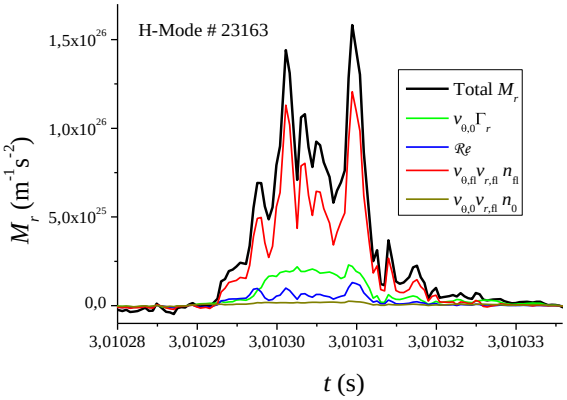

Fig. 3: Close up of the strong transport event shown in Fig. 2 by the red and blue lines. Total momentum (black line), the other lines show the parameters listed.

Again we see here that the total flux is mainly due to the triple fluctuating term $n_{fl}\, v_{r,fl}\, v_{\theta,fl}$.

These results in H-mode plasmas may be understood by taking account of the large external momentum input due to NBI into the core plasma. This momentum is subsequently transported into the SOL by the ELM filaments by a combination of convection and nonlinear transfer. However, the Reynolds stress, giving rise to conductive momentum flux, appears to be very small at least at the probe position.

This will be consistent with strong loss of poloidal momentum during each ELM event which appears compatible with the above discussed variation of poloidal and toroidal rotation during ELM events while the Reynolds stress appears to have no counteracting effect here. The question why the direction of momentum flux at the probe location is opposite between L- and H-mode cannot be answered as yet. A negative flux may be negative momentum transported outward or positive momentum inward. Whether these observed differences are a consequence of confinement regime or the presence of an external momentum source, needs further experimental investigation. In this connection we mention that in the L-mode the external momentum input is much weaker than in the H-mode. A more detailed evaluation of the experimental results will be presented in a forthcoming publication [6].

Acknowledgements

This work, supported by the European Communities under the Contracts of Associations between EURATOM and ÖAW, IPP, ENEA-RFX and RISØ-DTU, was carried out within the framework of the EFDA. The content of the publication is the sole responsibility of its authors and it does not necessarily represent the views of the Commission or its services. This work was also supported by grant P19901 of the Austrian Science Fund (FWF).

References

[1] T.W. Versloot, P.C. de Vries, C. Giroud, et al. Plasma Phys. Control. Fusion 52 045014 (2010).

[2] E.R. Solano, S. Jachmich, F. Villone, et al., Nucl. Fusion 48, 065005 (2008).

[3] C. Ionita, N. Vianello, H.W. Müller, et al., J. Plasma Fusion Res. Series 8, 413 (2009).

[4] N. Vianello, R. Schrittwieser, V. Naulin, et al., Europhys. Conf. Abstr. 33E, P1.166 (2009).

[5] J. R. Myra, D. A. Russell, D.A. D'Ippolito, Phys. Plasmas 15, 032304 (2008).

[6] F. Mehlmann, C. Ionita, V. Naulin, et al., in preparation.